IJP: Drugs and Drug Resistance 8 (2018) 295–303

Contents lists available at ScienceDirect

IJP: Drugs and Drug Resistance

journal homepage: www.elsevier.com/locate/ijpddr

Functional screening of selective mitochondrial inhibitors of *Plasmodium*

Maria G. Gomez-Lorenzo[a], Ane Rodríguez-Alejandre[a], Sonia Moliner-Cubel[a], María Martínez-Hoyos[a], Noemí Bahamontes-Rosa[a], Rubén Gonzalez del Rio[a], Carolina Ródenas[b], Jesús de la Fuente[b], Jose Luis Lavandera[a,c], Jose F. García-Bustos[a,d], Alfonso Mendoza-Losana[a,*]

[a] Diseases of the Developing World (DDW), Tres Cantos Medicine Development Campus, GlaxoSmithKline, Severo Ochoa 2, 28760, Tres Cantos, Madrid, Spain
[b] Centro de Investigación Básica (CIB) GlaxoSmithKline, Tres Cantos, Madrid, Spain
[c] Department of Basic Medical Science, CEU San Pablo University, Julián Romea 23, 28003, Madrid, Spain
[d] Department of Microbiology and Biomedicine Discovery Institute, Monash University, 3800, VIC, Australia

ARTICLE INFO

Keywords:
Plasmodium falciparum
Plasmodium yoelii
Oxygen consumption
Mitochondrial inhibitors and cytochrome

ABSTRACT

Phenotypic screening has produced most of the new chemical entities currently in clinical development for malaria, plus many lead compounds active against *Plasmodium falciparum* asexual stages. However, lack of knowledge about the mode of action of these compounds delays and may even hamper their future development. Identifying the mode of action of the inhibitors greatly helps to prioritise compounds for further development as novel antimalarials. Here we describe a whole-cell method to detect inhibitors of the mitochondrial electron transport chain, using oxygen consumption as high throughput readout in 384-well plate format. The usefulness of the method has been confirmed with the Tres Cantos Antimalarial Compound Set (TCAMS). The assay identified 124 respiratory inhibitors in TCAMS, seven of which were novel anti-plasmodial chemical structures never before described as mitochondrial inhibitors.

1. Introduction

Malaria is still one of the deadliest infectious diseases in the world (WHO, 2015). Several *Plasmodium* species can infect humans, and of these, *P. falciparum* causes the most severe form of the disease. Over the past 50 years, antimalarial chemotherapy has depended on just four classes of drugs: antifolates, endoperoxides, quinolines (4 and 8 amino quinolines) and quinolones. The inevitable emergence and spread of resistance to all four classes has created an urgent need for new drugs at affordable prices. There are several possible approaches to the discovery of new therapeutic compounds. A strategy employed by academic (e.g. Guiguemde et al., 2010) and industry (e.g. Gamo et al., 2010; e.g. Plouffe et al., 2008) laboratories is screening for *P. falciparum* growth inhibitors *in vitro*, an approach that has produced a wider structural diversity to date. The current challenge is to prioritise tens of thousands of hit compounds for future development, in order to identify the drug candidates most likely to be successful. If the primary biochemical mechanisms responsible for the observed anti-plasmodial activity are established in an efficient manner, compounds can be prioritised, classes with redundant mechanisms likely to be affected by cross-resistance can be identified, and progression can focus on modes of action considered desirable for their clinical validation or parasitological effects.

One of the few validated targets in *P. falciparum* is mitochondrial function (Painter et al., 2007). Extensive analyses of the data from parasite genome sequence projects and biochemical and physiological studies have revealed the presence of an active electron transport chain that can generate the electrochemical potential necessary for coenzyme Q and iron-sulphur cluster biosynthesis, as well as for pyrimidine metabolism (Painter et al., 2007; Vaidya and Mather, 2009; van Dooren et al., 2006). The latter seems to be the critically essential role of the canonical mitochondrial electron transport chain under *in vitro* conditions (Painter et al., 2007) and during the intraerythrocytic cycle *in vivo*. It should be noted however that other life stages seem to have expanded requirements for a functional respiratory chain in *Plasmodium* species (Hino et al., 2012; Sturm et al., 2015). It has been known for quite some time that this essential function is also highly druggable and can be selectively inhibited with compounds such as atovaquone (Fry and Pudney, 1992; Hudson, 1993) and the more recently described 4-(1H) pyridones (Capper et al., 2015; Cowley et al., 2012; Yeates et al., 2008).

However, the development of biochemical methods to measure *Plasmodium* mitochondrial function and inhibition with enough throughput to test tens of thousands of compounds under comparable conditions in a reasonable time presents numerous complications, including: (i) the difficulty of purifying functional mitochondria, which

* Corresponding author. C/ Severo Ochoa, 2, Tres Cantos, 28760, Madrid, Spain.
E-mail addresses: alfonso.x.mendoza@gsk.com, am11799@gsk.com (A. Mendoza-Losana).

https://doi.org/10.1016/j.ijpddr.2018.04.007
Received 17 October 2017; Received in revised form 20 April 2018; Accepted 26 April 2018
Available online 09 May 2018

underlies the low reproducibility between experiments from different laboratories; (ii) the low throughput of the techniques used, which traditionally require Clark-type electrodes or flow cytometry (Srivastava et al., 1997); and (iii) the intrinsically low *in vitro* respiratory rate of *P. falciparum* mitochondria, due to the parasite using the glycolytic pathway as its main source of metabolic energy during intraerythrocytic growth.

Here we describe a method capable of testing tens of thousands of compounds with whole-cell activity and identifying inhibitors of parasite mitochondrial metabolism by measuring oxygen consumption in red blood cells (RBCs) infected with *Plasmodium* species, using short incubation times and a high throughput format. The assay reliably differentiated compounds targeting the respiratory chain from those inhibiting *Plasmodium* growth through a different mechanism. The method has been validated using known mitochondrial inhibitors and standard antimalarial compounds and was used to identify novel inhibitors of the electron transport chain present in the TCAMS, set of phenotypic hits (Gamo et al., 2010).

2. Materials and methods

2.1. Biological material

Plasmodium yoelii 17XL was maintained *in vivo* in female CD1 mice. Four days after infection, blood from each mouse was collected in 4 ml of Hank's balanced solution (HBSS) containing 10 units of heparin/ml at approximately 50% parasitemia. Blood was washed three times with HBSS at 800 × g for 10 min. Cells were diluted 1:1 in HBSS and passed through a pre-washed small plasmodipur leukocyte-filter (Euro Diagnostica V. B.). Each filter was used to effectively remove leukocytes from a maximum of 15 ml of blood. The collected red blood cells (RBCs) were washed and resuspended again in HBSS. Infected erythrocytes were enriched by centrifugation over a solution of PBS with 70% (v/v) Percoll and 0.3 M glucose at 335 × g in a swinging bucket rotor for 45 min at room temperature. The interphase, containing trophozoites and schizonts almost exclusively, as determined by Giemsa-stained thin blood smears, was collected. Infected RBCs (iRBCs) were washed twice with RPMI 1640 medium containing 1% (v/v) foetal calf serum (FCS) and resuspended in the same medium at $7{\cdot}10^8$ iRBCs/ml for assays. During all these processes, unless otherwise noted, cells were maintained at 4 °C. All animal studies were ethically reviewed and carried out in accordance with European Directive 86/609/EEC and the GSK Policy on the Care, Welfare and Treatment of Animals. Guidelines and codes of conduct for animal care and research performed at the DDW Laboratory Animal Science facilities were approved and accredited by the American Association for Accreditation of Laboratory Animal Care (AAALAC).

3D7 and K1 strains of *P. falciparum* from MR4 (American Culture Type Collection) were grown in human type O + erythrocytes obtained from the Spanish Red Cross Blood Bank in complete medium: RPMI 1640 with 25 mM HEPES and $NaHCO_3$ (Sigma R5886), 20 mg/L hypoxanthine and 0.5% (v/v) Albumax II (Invitrogen) and grown in 5% CO_2, 5% O_2 and 90% N_2 at 37 °C. For each experiment, cultures of 250 ml at 4% haematocrit were grown in five 175 cm^2 flasks, with daily medium changes, and harvested at the highest possible trophozoite and schizont parasitemia (≥10%) by centrifugation at 800 × g at room temperature. iRBC were washed twice in RPMI containing 1% (v/v) FCS and adjusted in that media to $4{\cdot}10^8$ iRBCs/ml, 33% haematocrit. A total of $8.4{\cdot}10^7$ iRBC/well were used for screening and subsequent experiments, whereas different numbers *P. falciparum*-infected RBCs-well were used in the pilot experiments to develop the assay, as indicated in the *Oxygen consumption assay* section below and the legends to the figures. As mature forms (trophozoites and schizonts) are the most metabolically active and hence most likely to consume oxygen, cultures were harvested at time points when the proportion of mature forms was maximal (Supplementary Table 4).

Human epithelial HEK 293 cells were grown at 37 °C in SMEM (Sigma M8167) with 2 mM L-glutamine, 10% (v/v) FCS and 1% (w/v) Pluronic F127 (Sigma), using a continuous culture system. Cells were collected by centrifugation at 800 × g during 10 min at RT, washed twice in SMEM with 10% (v/v) FCS medium and then adjusted to $1.3{\cdot}10^7$ cells/ml.

2.2. Compounds

Atovaquone, endochin and TCAMS compounds (GSK), stigmatellin (Fluka), FCCP (Sigma) and proguanil (Molekula) were dissolved in DMSO. Sodium azide (Panreac), potassium cyanide (Sigma) and chloroquine (Sigma) in water and myxothiazol, antimycin and rotenone (Sigma) in ethanol. In the assay, the final concentration for DMSO or ethanol was 0.5% (v/v), a concentration that did not inhibit oxygen consumption and which was used as a 0% inhibition control (Control 1).

2.3. Oxygen consumption assay

To set up the assay, the first experiments with HEK 293, *P. yoelii* and *P. falciparum* cells were done in 96-well plates, to measure signal-to-background (S/B), timeframe needed to calculate Vmax and a starting point of the number of cells per well. As HEK 293 and *P. yoelii* were going to be used in a HTS campaign, assay was later set up in 384-well plate format. *P. falciparum* cells were only used in 96-well plates, as the amount of culture needed to observe oxygen consumption did not allow miniaturization the assay to 384-well plates.

Different amounts of cells were needed for each cell type to obtain the desired signal-to-noise ratio. $6.5{\cdot}10^5$ HEK 293 mammalian and $1.4{\cdot}10^7$ for *P. yoelii* iRBCs in 384-well plates and $8.4{\cdot}10^7$ iRBC for *P. falciparum* iRBCs in 96-well plates.

Plasmodium cells were incubated with the inhibitors at a wide range of concentrations for 20 min at 37 °C, and then transferred to the BD™ Oxygen Biosensor System (BD™ OBS) from BD Biosciences. 96-well (for *P. falciparum*) or 384-well (for *P. yoelii*). The pre-incubation step was introduced to reduce the lag-time observed when plates are incubated immediately following parasite addition. BD™ OBS plates were previously filled with RPMI 1640 medium, 1% (v/v) FCS, pre-warmed to 37 °C, to give a final volume of 200 µl (for 96-well plates) or 80 µl (for 384-well plate format), containing test compounds at the same concentration as in the pre-incubation step. HEK 293 cells were not pre-incubated to avoid losing adherent cells in this intermediate step, so they were directly seeded in the BD™ OBS plate that already had SMEM with 10% (v/v) FCS media and the inhibitors. The plates were placed in a Spectramax Gemini EM plate reader (Molecular Devices), and the fluorescence emitted at 630 nm was measured from the bottom, after excitation at 485 nm (cut-off of 495 nm), at 2 min intervals for HEK 293 and *P. yoelii*, or 5 min in the case of *P. falciparum*. Data were collected for 2 h for HEK 293 and *P. yoelii* and 12 h for *P. falciparum*. The intensity of fluorescence in each well correlates with the oxygen concentration present at each measurement. The V_{max}, expressed as the increase in fluorescence over time, was automatically calculated as the slope at the inflection point of the sigmoidal graph using 10 points in the case of HEK 293 and *P. yoelii* or 50 points for *P. falciparum*. The initial slope was constant between 8 and 50 min for HEK 293, between 30 and 90 min for *P. yoelii* and between 30 min and 8 h for *P. falciparum*. Percent inhibition by a compound concentration was calculated relative to the 0.5% DMSO (0% inhibition of oxygen consumption, Control 1) after subtracting the background fluorescence in wells treated with 1.25 µM atovaquone (100% inhibition oxygen consumption, Control 2) in the case of *Plasmodium* cells or stigmatellin at 10 µM for HEK 293 cells.

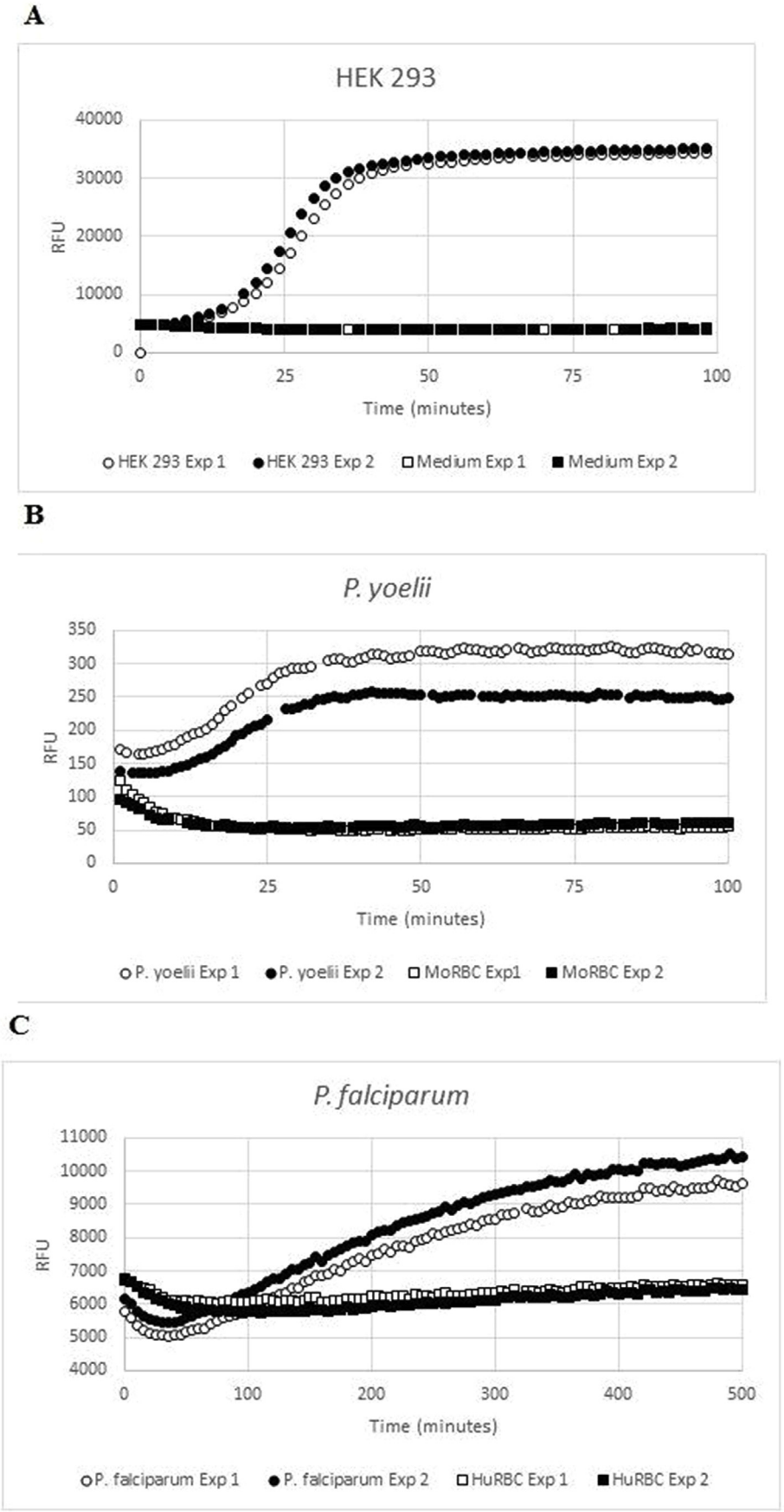

Fig. 1. Two replicates of one biological sample from each cell type showing changes in fluorescence emitted at 630 nm after excitation at 485 nm in a 96-well BD™ OBS plate with **(A)** $5{\cdot}10^6$ HEK 293 cells (circles), (**B**) $4.4{\cdot}10^7$ infected mouse RBCs with *P. yoelii* (circles) and mouse RBCs (MoRBC, squares) and (**C**) $1.3{\cdot}10^8$ *P. falciparum* iRBCs (circles) or human RBC (HuRBC, squares). HEK 293 and *P. yoelii* samples were measured every 2 min and *P. falciparum* every 5 min.

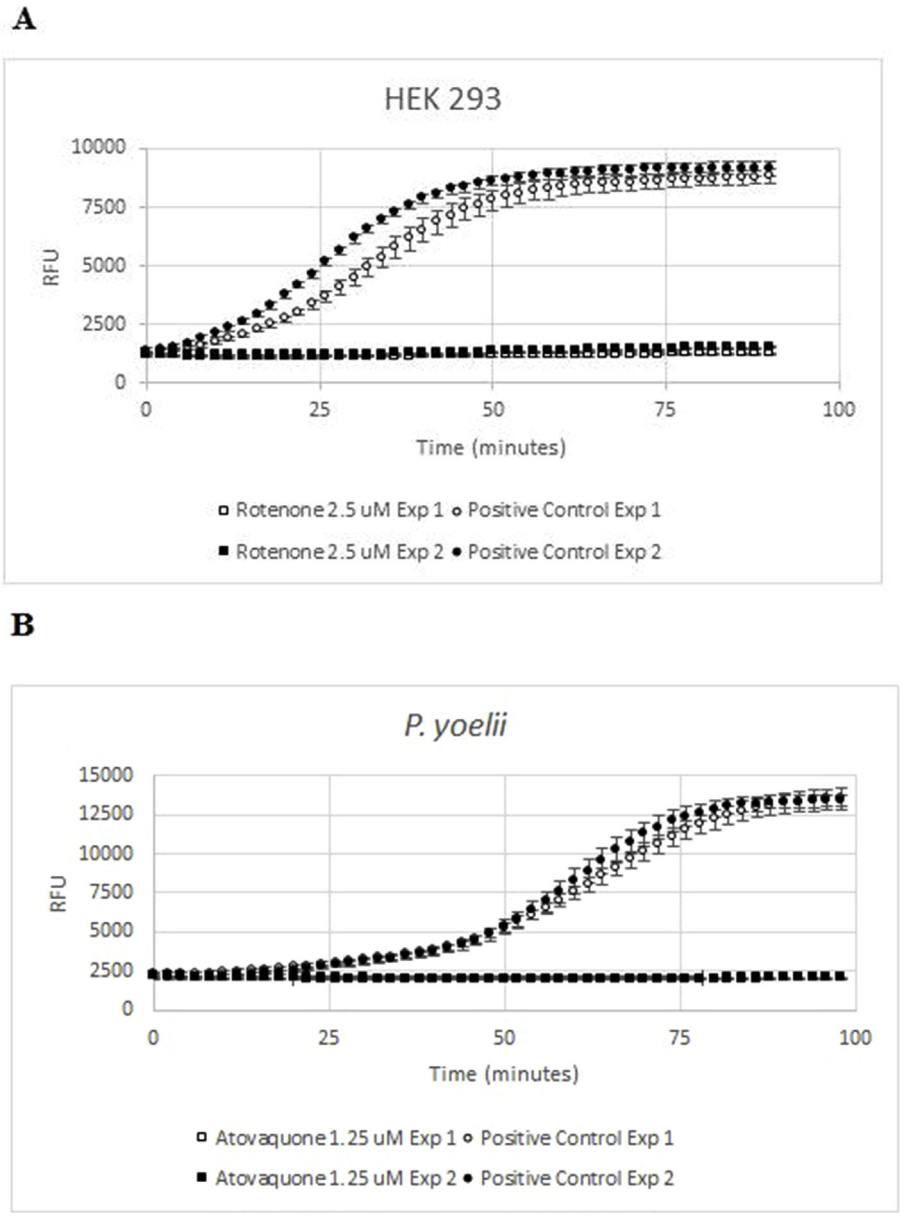

Fig. 2. Inhibition of oxygen consumption by incubation with inhibitors. Two experiments performed in different days, with technical quadruplicates, are shown, with the corresponding average and standard deviation for each experiment and time-point. Squares show inhibition with inhibitors while circles are positive controls. (**A**) Incubation of $6.5{\cdot}10^5$ HEK 293 cells with rotenone at 2.5 μM, (**B**) $2{\cdot}10^7$ *P. yoelli* cells with 1.25 μM atovaquone.

2.4. TCAMS screening in P. yoelii

P. yoelii cells were used for the primary screening of the 13,103 compounds in the TCAMS identified as growth inhibitors of *P. falciparum* in a screen of nearly two million compounds from the GSK corporate collection (Gamo et al., 2010). 50 nL of 10 mM compound were dispensed in 384-well plates, leaving columns 6 and 18 for positive (DMSO) and negative (atovaquone 1.25 μM, final concentration) controls, respectively. Compounds were initially tested at a single concentration of 2 μM. The percent of inhibition for each well in the plate was calculated considering the averages (AVG) of positive and negative controls producing 100% and 0% inhibition respectively. Robust mean, 91%, and standard deviation (SD), 19%, of all wells tested in the screening, excluding negative controls, were used to calculate the cut-off (robust mean - 3*SD) (Analytical Methods Committee, 1989). To estimate compound selectivity dose/response curves were generated for hits inhibiting oxygen consumption by more than 65% at 2 μM, in order to calculate their IC_{50} in *P. yoelii* and HEK 293 cells in parallel, using replicates of master plates. In this case, the 100% inhibition control was stigmatellin at 10 μM; this compound inhibits oxygen consumption in *Plasmodium* spp and mammalian cells. For the IC_{50} determination experiments, 11 serial 1/3 dilutions starting at 20 μM (the concentration in the single-point assay) were used and values reported as the average of at least two biological replicates, using parasites prepared in different days. IC_{50} determinations were considered valid only if the plate Z' values were higher than 0.4. Statistics for IC_{50} determination are summarized in Supplementary Table 3.

2.5. Chemical clustering

Chemical clusters in the TCAMS were identified following two approaches. Firstly, structural core templates were identified from those initial hits and classified in 416 different chemical frameworks. Secondly, fingerprint clusters annotations were also calculated using

Daylight (Daylight Chemical Information Systems, 2008) fingerprint methods used a Tanimoto similarity index of 0.85, in order to extract distinct classes from within the broader molecular framework categories. As a result, those initial chemical frameworks were subdivided in different clusters depending on substituent patterns. Finally, analysis of the biological data associated to each cluster was performed with SpotfireDecisionSite 8.2.1 software and Microsoft Excel.

2.6. Enzymatic cytbc1 activity

Mitochondria from *P. falciparum* K1 strain were isolated after nitrogen cavitation of iRBC, differential centrifugation and sucrose density gradient purification, and then stored at −80 °C at 40 μg/ml concentration. Ubiquinol: cytochrome *c* oxidoreductase activity was measured as the antimycin-sensitive cytochrome *c* reduction by decylubiquinol in isolated mitochondria at 40 μg/ml concentration, as detailed in (da Cruz et al., 2012). Compounds were tested at 0.5 μM and 5 μM and atovaquone was used as 100% inhibition control. The percentage of inhibition at each concentration was calculated as above.

3. Results

3.1. Assay development

The assay relies on BD™ OBS plates, which have a silicone base that incorporates a fluorophore quenched by molecular oxygen in a quantitative manner. When cell respiration removes oxygen from the medium, fluorescence at 630 nm increases (excitation wavelength 485 nm). Thus, positive (no-inhibition) controls consume oxygen at the maximum rate and produce the highest fluorescence values, while negative (no-respiration) controls display the lowest values, and wells in which cells are incubated with respiratory chain inhibitors produce fluorescence readouts indicative of the level of oxygen consumption (Fig. 1).

Exploratory assays for HEK 293, *P. yoelli* and *P. falciparum* cells were done in 96-well plates. First, experiments using $5{\cdot}10^6$ HEK 293 cells/well (Fig. 1A) were done to observe the increase in fluorescence with incubation time. Then, $4.4{\cdot}10^7$ *P. yoelii* cells, compared to mouse RBCs from uninfected animals (Fig. 1B), and $1.3{\cdot}10^8$ *P. falciparum* cells compared to the same number of uninfected human RBCs were tested (Fig. 1C). No oxygen consumption signal was detected from uninfected RBCs, either from mouse or human. In all cases, incubation of all nucleated cells in a well of a BD™ OBS plate displayed a marked increase in fluorescence over time, indicating that mammalian cells and *Plasmodium* parasites were consuming the oxygen dissolved in the medium (Fig. 1A–C). This signal was completely inhibited by the addition of rotenone in HEK 293 cells (Fig. 2A) or atovaquone in *Plasmodium* cells (Fig. 2B), well-known electron transport inhibitors of mammalian and plasmodial cells respectively (Uyemura et al., 2004; Srivastava et al., 1997; van Dooren et al., 2006). This result also indicates that there is no signal coming from a potential contamination with rodent leukocytes in the *P. yoelii* assay. The signal-to-noise ratio was higher than five. This result showed that BD™ OBS plates are a suitable tool for measuring oxygen consumption in mammalian and *Plasmodium* cells and hence for analysing mitochondrial respiration. As the final aim of this work was to run a high throughput screen, miniaturization to 384-well plate format was undertaken for HEK 293 and *P. yoelii* cells.

When different numbers of *P. yoelii* iRBCs were incubated in the BD™ OBS 384-well plate, the rate of oxygen consumption (V_{max}) increased linearly with the number of parasites/well, with correlation coefficients (R^2) higher than 0.98 (Fig. 3A), and $1.4{\cdot}10^7$ iRBC/well in 384-well plates was considered an optimum cell number for further assays.

P. falciparum cells were also found to give a robust signal using this methodology, although the assay required much longer incubation times and gave lower V_{max} values (Fig. 1C). When dilutions of the human parasite were tested, the amount of oxygen consumed was found to increase linearly with parasite number, albeit with a smaller slope than when using *P. yoelii*, confirming that *P. falciparum* cells consume less oxygen than the rodent parasites *in vitro* (Fig. 3B).

3.2. Assay validation

Once the above experimental conditions were set, the assay was validated using chloroquine and atovaquone, two potent antimalarial drugs that inhibit different cellular pathways, and rotenone, a well-known inhibitor of the mammalian respiratory complex I (Hatefi, 1978) with poor anti-plasmodial activity. As expected, chloroquine, a quick-acting drug that interferes with parasite hemozoin formation, did not show any effect on oxygen consumption by either parasite species during the time of the experiment (IC_{50} greater than 12 μM), whereas atovaquone, a slow parasite killer but efficient inhibitor of mitochondrial function in *Plasmodium* (Fry and Beesley, 1991; Fry and Pudney, 1992; Hudson, 1993), displayed a clear inhibitory effect on oxygen consumption with potencies in the nM range (Table 1), both in a drug-sensitive strain, 3D7, as well as in a chloroquine-resistant background, K1. As expected, neither *Plasmodium* species was significantly inhibited by rotenone, since they lack respiratory complex I and the existing alternative NADH: ubiquinone oxidoreductase, a type II (non-proton pumping) dehydrogenase, is insensitive to the drug (Biagini et al., 2006; Srivastava et al., 1997; Uyemura et al., 2004).

HEK 293 cells were used to evaluate the ability of the assay to detect compound selectivity, using $6.5{\cdot}10^5$ cells/well in 384-well plate format. These cells consume oxygen much faster than *Plasmodium* parasites, allowing the use of lower cell numbers and shorter incubation times to obtain IC_{50} values. No inhibition of respiration was observed when HEK 293 cells were incubated with atovaquone or chloroquine, while it was clearly inhibited by rotenone as expected (Hatefi, 1978) (Table 1).

3.3. Effect of standard inhibitors of the electron transport chain

Once the assay conditions were optimized and selectivity observed, different classical inhibitors of respiratory complexes III and IV, a membrane uncoupler (FCCP) and proguanil, a strong potentiator of atovaquone action through unknown mechanisms, were tested in the assay. Results, summarized in Table 2, show that proven complex III inhibitors binding at either Qo or Qi sites, such as antimycin, myxothiazol, stigmatellin, and endochin, all potently inhibited oxygen consumption, with endochin as the only compound selectively active against the parasites. Complex IV inhibitor potassium cyanide shows a high IC_{50} against the parasites, while the uncoupler FCCP is uniformly, albeit relatively weakly active in the assay.

3.4. Screening of the TCAMS using the oxygen consumption assay

We tested 13,103 compounds of the TCAMS using *P. yoelii* and HEK 293 cells in 384-well plate format with $1.4{\cdot}10^7$ *P. yoelii* iRBC/well, in what we have called the oxygen consumption assay (OCA). The first set of experiments was performed at a single concentration of 2 μM and 149 compounds showed an inhibition of more than 65% (cut-off value described in Materials and Methods). Their IC_{50} was measured in *P. yoelii* and HEK 293 cells to compare potency and selectivity. Results are summarized in Table 3 and Supplementary Table 1. The robustness of the screen was supported by the fact that all the 4-(1H) pyridones, quinolones and their derivatives (91 in total) present in TCAMS were identified as positives in the assay. Twenty-five compounds were not oxygen consumption inhibitors when re-tested and were considered false positives. All compounds displayed a degree of selectivity, with IC_{50} higher than 5 μM in HEK 293 cells.

Moreover, the degree of correlation between the IC_{50} for *P. yoelii* oxygen consumption in TCAMS and the published potency in *P. falciparum* growth inhibition (XC_{50}) (Gamo et al., 2010) was calculated

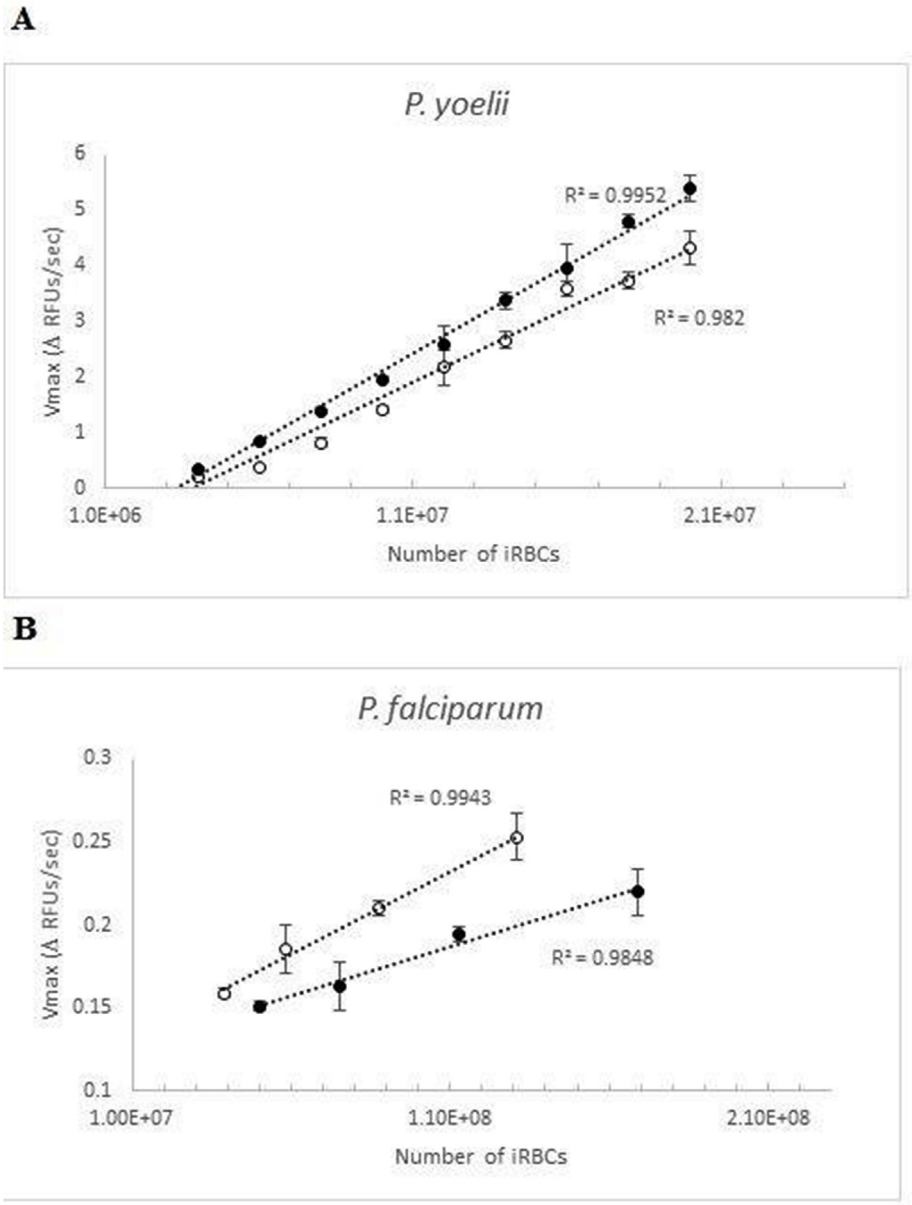

Fig. 3. Linear correlation between numbers of (**A**) *P. yoelii* or (**B**) *P. falciparum* parasites and the rate of oxygen consumption, Vmax, expressed as the increment in fluorescence over time. Two experiments, done in different days, are shown with technical quadruplicates for *P. yoelii* cells in p386-well plates and duplicates with *P. falciparum* cells in 96-well plates. Average and standard deviation for each number of cells tested are shown.

Table 1
IC_{50} values (μM) for the Oxygen Consumption Assay for atovaquone, chloroquine and rotenone.

Compound	IC_{50} values (μM) for the Oxygen Consumption Assay				[a]AWC XC_{50} values (μM)
	P. yoelii (17XL)	*P. falciparum* (K1)	*P. falciparum* (3D7)	*H. sapiens* (HEK 293)	*P. falciparum* (3D7)
Atovaquone	0.005 ± 0.001 (n = 27)	0.0013 ± 0.0008 (n = 10)	0.0011 ± 0.0006 (n = 36)	> 6 (n = 44)	0.001
Chloroquine	> 12 (n = 6)	> 12 (n = 4)	> 12 (n = 2)	> 12 (n = 2)	0.08
Rotenone	> 2.5 (n = 3)	> 2.5 (n = 2)	ND	0.026 ± 0.011 (n = 4)	27

[a] *P. falciparum* growth inhibition published by (Gamo et al., 2010).

(Supplementary Fig. 1). Overall correlation between the two parasites, represented by the square of the coefficient of correlation (R^2) is poor (e.g. 0.41 for quinolone cluster), with compounds tending to be more potent at inhibiting *P. falciparum* growth than *P. yoelii* respiration, perhaps not surprising since the compounds were first identified as *P. falciparum* inhibitors. The ideal scenario would have been to directly compare oxygen consumption and growth inhibition in *P. yoelii*, but whole cell data in this parasite for the TCAMS compounds is lacking.

Table 2
Effect of standard inhibitors of the electron transport chain in OCA.

IC_{50} values (μM) for the Oxygen Consumption Assay				
	P. falciparum (K1)	*H. sapiens* (HEK 293)	*P. yoelii* (17 XL)	Selectivity (*P. falciparum vs H. sapiens*)
Sodium azide	> 500 (n = 4)	243 (n = 4)	810 (n = 3)	< 0.48
Antimycin	0.016 ± 0.008 (n = 9)	0.006 ± 0.001 (n = 4)	0.010 + 0.003 (n = 3)	0.375
Endochin	0.088 ± 0.024 (n = 6)	> 25 (n = 4)	0.011 + 0.005 (n = 3)	284
Stigmatellin	3.64 ± 1.78 (n = 12)	0.058 ± 0.051 (n = 19)	0.094 + 0.049 (n = 4)	0.015
FCCP	18.3 ± 1.31 (n = 4)	35.4 + 22.7 (n = 4)	8.60 + 0.28 (n = 4)	1.93
Potassium cyanide	1610 ± 1340 (n = 4)	147 ± 40 (n = 4)	599 + 182 (n = 3)	0.09
Myxothiazol	0.41 ± 0.28 (n = 12)	0.029 ± 0.012 (n = 4)	0.20 + 0.06 (n = 3)	0.07
Proguanil	> 10 (n = 4)	> 10 (n = 4)	> 12 (n = 1)	–

Table 3
Range of IC_{50} potencies measured in the oxygen consumption assay with *P. yoelii* and HEK 293 cells.

Number of compounds	IC_{50} in *P. yoelii* (μM)	IC_{50} in HEK 293 (μM)
25	> 10	> 5
18	1–10	> 5
93	0.1–1	> 5
13	< 0.1	> 5

Otherwise, the same comparison could have been done in *P. falciparum*, but TCAMS screening in oxygen consumption assay has technical limitations that could not be overcame. So, either way, it is not possible to compare data from both assays in the same species.

The short incubation time of the assay was chosen in order to identify the primary mode of action of the compounds, independently of the speed at which they can irreversibly block parasite replication. This was confirmed with atovaquone, a slow-killing compound with fast inhibition of respiration, and chloroquine or mefloquine, fast killers without activity in the respiration assay described here, plus a set of compounds from TCAMS with previously measured *in vitro* parasite reduction rates (see Supplementary Table 2) (Linares et al., 2015).

3.5. All novel respiration blockers are cytbc1 inhibitors

In order to test which, if any, of the novel respiratory inhibitors acted through the highly druggable cytbc1 function, mitochondrial extracts from *P. falciparum* were prepared and an enzymatic assay was performed using two different compound concentrations, 5 μM and 0.5 μM, with atovaquone as control. All the new scaffolds identified showed significant cytbc1 inhibition in the cell-free assay (Table 4), making it highly likely that this cytochrome is the primary target of the novel compounds.

4. Discussion

Our results describe a methodology with a high degree of specificity for identifying respiratory inhibitors in a whole-cell, high-throughput format. Assay specificity was demonstrated by its ability to clearly distinguish atovaquone, a known inhibitor of mitochondrial function in *Plasmodium*, from chloroquine, a well-known, fast-acting and potent anti-plasmodial with an unrelated mechanism of action (Fry and Pudney, 1992; Hudson, 1993). The link between inhibition of the parasite respiratory complexes and a decrease in oxygen consumption by iRBCs was established using respiratory inhibitors of different specificities. Rotenone, which targets the complex I absent from these parasites, was scored as a negative. Known inhibitors of parasite complex III, such as atovaquone, antimycin, stigmatellin or myxothiazol, were clear positives. These results are in line with mitochondrial physiology results from different laboratories (Fry and Beesley, 1991; Srivastava et al., 1997; Takashima et al., 2001; Uyemura et al., 2000, 2004). However, not all complex III inhibitors showed the same species selectivity. Atovaquone and endochin have a clear anti-parasitic selectivity profile, with more than three orders of magnitude difference in potency between the parasite and mammalian cells. The other three compounds tested, myxothiazol, antimycin and stigmatellin, are not strictly selective but parasite mitochondria have different sensitivities compared to mammalian ones. Proguanil does not inhibit oxygen consumption at any concentration tested, in line with previous studies in which no effect on electron transport or mitochondrial membrane potential could be detected (Srivastava and Vaidya, 1999), despite the well-known synergy of this compound with atovaquone (Painter et al., 2007), which is independent of its activity as an antifolate pro-drug (Boggild et al., 2007).

Our results confirmed that the assay could measure *Plasmodium* respiration rates in intact parasites and differentiate between respiratory inhibitors and antimalarials with alternative modes of action. Data obtained with the 13,103 TCAMS anti-plasmodial compounds showed that 1% affected oxygen consumption, including 7 novel chemical classes not previously described as electron transport inhibitors. They all seem to target cytbc1, confirming respiratory complex III as the most tractable target in the electron transport chain. The reasons for this high druggability are not specifically known and we can only speculate. Any enzyme with growth-limiting activity and whose natural substrates or effectors have physico-chemical properties overlapping those in corporate compound libraries would fulfil the definition of a highly tractable target. X-ray structures of the yeast Qo site in the cytbc1 complex bound to atovaquone, together with the mapping of point mutations conferring atovaquone resistance in *Plasmodium* and *Pneumocystis* (Birth et al., 2014; Kessl et al., 2004; Siregar et al., 2015), would support the view that cytbc1 inhibitors essentially need to possess a “warhead” able to undergo redox cycling, linked to a hydrophobic tail capable of establishing some of the interactions that naturally hold in place the flexible isoprenoid chain of ubiquinone. This does not impose a lot of structural constrain, other than having a minimum size to span from the functional groups involved in electron transport to the hydrophobic patches at the other end of the Qo site. The required lipophilic moieties in the inhibitors probably also facilitate their penetration through biological membranes, increasing their representation among hits from phenotypic screens.

Table 4
Chemical entities not described before as mitochondrial inhibitors.

Compounds	Structure	OCA *P. yoelii*		OCA HEK 293		[a]*P. falciparum* AWC	% Inhibition Cytbc1 biochemical assay		
		IC_{50} (μM)	n	IC_{50} (μM)	n	XC_{50} (μM)	5 μM	0.5 μM	n
TCMDC-134575	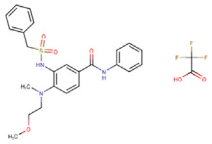	0.514 ± 0.225	3	> 10	3	0.571	91.48 ± 7.57	56.25 ± 7.06	3
TCMDC-123689	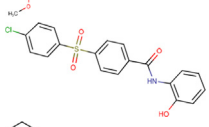	8.190 ± 1.260	3	> 10	2	1.345	99.84 ± 2.22	65.48 ± 7.02	3
TCMDC-124874	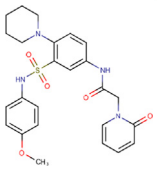	0.760 ± 0.109	3	> 10	2	0.695	59.97 ± 8.70	14.61 ± 2.05	3
TCMDC-124578	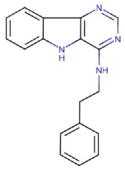	0.292 ± 0.249	3	7.521 ± 0.500	3	0.600	100.30 ± 2.14	63.85 ± 2.65	3
TCMDC-134937	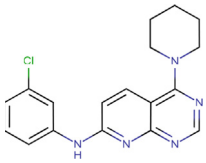	1.319 ± 0.860	3	> 10	2	0.577	50.34 ± 6.78	4.76 ± 9.24	2
TCMDC-133823	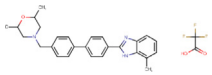	2.201 ± 1.950	3	> 10	3	0.522	89.93 ± 9.67	48.96 ± 1.05	2
TCMDC-125039	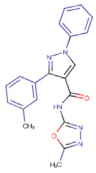	1.096 ± 0.131	2	> 10	2	1.160	77.11 ± 12.20	47.90 ± 7.35	2
Atovaquone	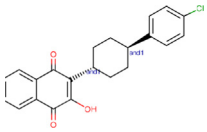	0.005 ± 0.001	27	> 6	44	0.001	101.02 ± 9.82	105.41 ± 8.26	2

[a] *P. falciparum* Whole Cell Time Extended 72 h (Gamo et al., 2010).

Although *P. yoelii* proved to be a good *P. falciparum* surrogate in this assay, it also highlighted differences between human and rodent parasites, the most obvious being the much higher respiration rates of the rodent parasites and their higher sensitivity to stigmatellin. These results reinforce the need for *P. falciparum* animal models in anti-malarial drug development, to confirm compound activity against the disease-relevant parasite in an *in vivo* setting (Angulo-Barturen et al., 2008).

A genetically modified *P. falciparum* strain overexpressing yeast DHODH could have been used to develop an alternative assay to the screening format employed here, although we found the OCA to present some advantages. It does not rely on any single *Plasmodium* species and it is not restricted to a given genetic background, therefore the assay can be applied to any *Plasmodium* spp. isolate, for instance *P. vivax*. Furthermore, the assay measures a physiological function that is common between phylogenetically distant organisms and the results can be compared side by side to assess specificity.

The assay described herein has been used in the progression of different 4-(1H) pyridone derivatives at GSK (Bueno et al., 2011), all cytbc1 inhibitors. It has also proven instrumental in identifying new chemical leads from the TCAMS capable of acting on the well-validated *Plasmodium* electron transport chain targets.

5. Conclusion

Here we describe a whole-cell method to detect/identify inhibitors of the mitochondrial electron transport chain, using oxygen consumption as surrogate of mitochondrial function, in a high throughput 384-well plate format. The assay identified 124 respiratory inhibitors in the TCAMS, seven of which were novel anti-plasmodial chemical structures/chemotypes that greatly increase the number of known mitochondrial inhibitors.

Animal care and biological samples

All animal studies were ethically reviewed and carried out in

accordance with European Directive 2010/63/EU and the GSK Policy on the Care, Welfare and Treatment of Animals.

Human biological samples were sourced ethically and their research use was in accordance with the terms of the informed consents from donors.

Funding

We are grateful to MMV for financial support.

Acknowledgements

We are grateful to M[a] Jose Lafuente Monasterio for her collaboration in the cytbc1 assay.

In memoriam of Carmen Bravo.

Abbreviations

FCCP	carbonyl cyanide 4-(trifluoromethoxy)phenylhydrazone
IC50	concentration needed to produce 50% of inhibition at 48 h
XC50	estimated concentration needed to reach 50% inhibition in an *in vitro* P. falciparum whole cell assay at 72 h and generating dose–response curves using an interplate design ()
RBC	red blood cell
iRBC	red blood cell infected with Plasmodium
cytbc1	cytochrome *bc*1
OCA	oxygen consumption assay
AWC	antimalarial *in vitro* whole cell activity (inhibition) for P. falciparum
DMSO	dimethyl sulfoxide
TCAMS	Tres Cantos Antimalarial Set
SMEM	Minimum Essential Medium Eagle
HTS	High Throughput Screening
AVG	average
SD	Standard Deviation
S/B	Signal to Background
CV	Coefficient of Variation
HBA	H-bond acceptor count
HBD	H-bound donor count

Appendix A. Supplementary data

Supplementary data related to this article can be found at http://dx.doi.org/10.1016/j.ijpddr.2018.04.007.

References

Analytical Methods Committee, 1989. Robust statistics-how not to reject outliers. Part 1. Basic concepts. Analyst 114, 1693–1697.

Angulo-Barturen, I., Jimenez-Diaz, M.B., Mulet, T., Rullas, J., Herreros, E., Ferrer, S., Jimenez, E., Mendoza, A., Regadera, J., Rosenthal, P.J., Bathurst, I., Pompliano, D.L., Gomez de las, H.F., Gargallo-Viola, D., 2008. A murine model of falciparum-malaria by in vivo selection of competent strains in non-myelodepleted mice engrafted with human erythrocytes. PLoS One 3, e2252.

Biagini, G.A., Viriyavejakul, P., O'Neill, P.M., Bray, P.G., Ward, S.A., 2006. Functional characterization and target validation of alternative complex I of Plasmodium falciparum mitochondria. Antimicrob. Agents Chemother. 50, 1841–1851.

Birth, D., Kao, W.C., Hunte, C., 2014. Structural analysis of mitochondrial cytochrome bc1 complex with atovaquone bound reveals the molecular basis of antimalarial drug action. Malar. J. 13, S41.

Boggild, A.K., Parise, M.E., Lewis, L.S., Kain, K.C., 2007. Atovaquone-proguanil: report from the CDC expert meeting on malaria chemoprophylaxis (II). Am. J. Trop. Med. Hyg. 76, 208–223.

Bueno, J.M., Manzano, P., Garcia, M.C., Chicharro, J., Puente, M., Lorenzo, M., Garcia, A., Ferrer, S., Gomez, R.M., Fraile, M.T., Lavandera, J.L., Fiandor, J.M., Vidal, J., Herreros, E., Gargallo-Viola, D., 2011. Potent antimalarial 4-pyridones with improved physico-chemical properties. Bioorg. Med. Chem. Lett 21, 5214–5218.

Capper, M.J., O'Neill, P.M., Fisher, N., Strange, R.W., Moss, D., Ward, S.A., Berry, N.G., Lawrenson, A.S., Hasnain, S.S., Biagini, G.A., Antonyuk, S.V., 2015. Antimalarial 4(1H)-pyridones bind to the Qi site of cytochrome bc1. Proc. Natl. Acad. Sci. U. S. A 112, 755–760.

Cowley, R., Leung, S., Fisher, N., Al-Helal, M., Berry, N.G., Lawrenson, A.S., Sharma, R., Shone, A.E., Ward, S.A., Biagini, G.A., O'Neill, P.M., 2012. The development of quinolone esters as novel antimalarial agents targeting the Plasmodium falciparum bc1 protein complex. MedChemComm 3, 39–44.

da Cruz, F.P., Martin, C., Buchholz, K., Lafuente-Monasterio, M.J., Rodrigues, T., Sonnichsen, B., Moreira, R., Gamo, F.J., Marti, M., Mota, M.M., Hannus, M., Prudencio, M., 2012. Drug screen targeted at Plasmodium liver stages identifies a potent multistage antimalarial drug. J. Infect. Dis. 205, 1278–1286.

Fry, M., Beesley, J.E., 1991. Mitochondria of mammalian Plasmodium spp. Parasitology 102 (Pt 1), 17–26.

Fry, M., Pudney, M., 1992. Site of action of the antimalarial hydroxynaphthoquinone, 2-[trans-4-(4'-chlorophenyl) cyclohexyl]-3-hydroxy-1,4-naphthoquinone (566C80). Biochem. Pharmacol. 43, 1545–1553.

Gamo, F.J., Sanz, L.M., Vidal, J., de, C.C., Alvarez, E., Lavandera, J.L., Vanderwall, D.E., Green, D.V., Kumar, V., Hasan, S., Brown, J.R., Peishoff, C.E., Cardon, L.R., Garcia-Bustos, J.F., 2010. Thousands of chemical starting points for antimalarial lead identification. Nature 465, 305–310.

Guiguemde, W.A., Shelat, A.A., Bouck, D., Duffy, S., Crowther, G.J., Davis, P.H., Smithson, D.C., Connelly, M., Clark, J., Zhu, F., Jimenez-Diaz, M.B., Martinez, M.S., Wilson, E.B., Tripathi, A.K., Gut, J., Sharlow, E.R., Bathurst, I., El, M.F., Fowble, J.W., Forquer, I., McGinley, P.L., Castro, S., Angulo-Barturen, I., Ferrer, S., Rosenthal, P.J., Derisi, J.L., Sullivan, D.J., Lazo, J.S., Roos, D.S., Riscoe, M.K., Phillips, M.A., Rathod, P.K., Van Voorhis, W.C., Avery, V.M., Guy, R.K., 2010. Chemical genetics of Plasmodium falciparum. Nature 465, 311–315.

Hatefi, Y., 1978. Preparation and properties of NADH: ubiquinone oxidoreductase (complexI), EC 1.6.5.3. Methods Enzymol. 53, 11–14.

Hino, A., Hirai, M., Tanaka, T.Q., Watanabe, Y.I., Matsuoka, H., Kita, K., 2012. Critical roles of the mitochondrial complex II in oocyst formation of rodent malaria parasite Plasmodium berghei. J. Biochem. 152, 259–268.

Hudson, A.T., 1993. Atovaquone - a novel broad-spectrum anti-infective drug. Parasitol. Today 9, 66–68.

Kessl, J.J., Hill, P., Lange, B.B., Meshnick, S.R., Meunier, B., Trumpower, B.L., 2004. Molecular basis for atovaquone resistance in Pneumocystis jirovecii modeled in the cytochrome bc1 complex of Saccharomyces cerevisiae. J. Biol. Chem. 279, 2817–2824.

Linares, M., Viera, S., Crespo, B., Franco, V., Gomez-Lorenzo, M.G., Jimenez-Diaz, M.B., Angulo-Barturen, I., Sanz, L.M., Gamo, F.J., 2015. Identifying rapidly parasiticidal anti-malarial drugs using a simple and reliable in vitro parasite viability fast assay. Malar. J. 14, 441.

Painter, H.J., Morrisey, J.M., Mather, M.W., Vaidya, A.B., 2007. Specific role of mitochondrial electron transport in blood-stage Plasmodium falciparum. Nature 446, 88–91.

Plouffe, D., Brinker, A., McNamara, C., Henson, K., Kato, N., Kuhen, K., Nagle, A., Adrian, F., Matzen, J.T., Anderson, P., Nam, T.G., Gray, N.S., Chatterjee, A., Janes, J., Yan, S.F., Trager, R., Caldwell, J.S., Schultz, P.G., Zhou, Y., Winzeler, E.A., 2008. In silico activity profiling reveals the mechanism of action of antimalarials discovered in a high-throughput screen. Proc. Natl. Acad. Sci. U. S. A 105, 9059–9064.

Siregar, J.E., Kurisu, G., Kobayashi, T., Matsuzaki, M., Sakamoto, K., Mi-ichi, F., Watanabe, Y.I., Hirai, M., Matsuoka, H., Syafruddin, D., Marzuki, S., Kita, K., 2015. Direct evidence for the atovaquone action on the Plasmodium cytochrome bc1 complex. Parasitol. Int. 64, 295–300.

Srivastava, I.K., Vaidya, A.B., 1999. A mechanism for the synergistic antimalarial action of atovaquone and proguanil. Antimicrob. Agents Chemother. 43, 1334–1339.

Srivastava, I.K., Rottenberg, H., Vaidya, A.B., 1997. Atovaquone, a broad spectrum antiparasitic drug, collapses mitochondrial membrane potential in a malarial parasite. J. Biol. Chem. 272, 3961–3966.

Sturm, A., Mollard, V., Cozijnsen, A., Goodman, C.D., McFadden, G.I., 2015. Mitochondrial ATP synthase is dispensable in blood-stage Plasmodium berghei rodent malaria but essential in the mosquito phase. Proc. Natl. Acad. Sci. U.S.A. 112, 10216–10223.

Takashima, E., Takamiya, S., Takeo, S., Mi-ichi, F., Amino, H., Kita, K., 2001. Isolation of mitochondria from Plasmodium falciparum showing dihydroorotate dependent respiration. Parasitol. Int. 50, 273–278.

Uyemura, S.A., Luo, S., Moreno, S.N., Docampo, R., 2000. Oxidative phosphorylation, Ca (2+) transport, and fatty acid-induced uncoupling in malaria parasites mitochondria. J. Biol. Chem. 275, 9709–9715.

Uyemura, S.A., Luo, S., Vieira, M., Moreno, S.N., Docampo, R., 2004. Oxidative phosphorylation and rotenone-insensitive malate- and NADH-quinone oxidoreductases in Plasmodium yoelii yoelii mitochondria in situ. J. Biol. Chem. 279, 385–393.

Vaidya, A.B., Mather, M.W., 2009. Mitochondrial evolution and functions in malaria parasites. Annu. Rev. Microbiol. 63, 249–267.

van Dooren, G.G., Stimmler, L.M., McFadden, G.I., 2006. Metabolic maps and functions of the Plasmodium mitochondrion. FEMS Microbiol. Rev. 30, 596–630.

WHO (World Health Organization), 2015. World malaria report. http://www.who.int/malaria/publications/world-malaria-report-2015/report/en/.

Yeates, C.L., Batchelor, J.F., Capon, E.C., Cheesman, N.J., Fry, M., Hudson, A.T., Pudney, M., Trimming, H., Woolven, J., Bueno, J.M., Chicharro, J., Fernandez, E., Fiandor, J.M., Gargallo-Viola, D., Gomez de las, H.F., Herreros, E., Leon, M.L., 2008. Synthesis and structure-activity relationships of 4-pyridones as potential antimalarials. J. Med. Chem. 51, 2845–2852.